K. C. Oliveira, M. C. Cavalcanti, João L. Afonso, A. M. Farias, F. A. S. Neves, “Transformerless Photovoltaic Systems Using Neutral Point Clamped Multilevel Inverters”, Proceedings of ISIE 2010 - 2010 IEEE International Symposium on Industrial Electronics, Bari, Italy, 4-7 July 2010, pp. 1131-1136, ISBN: 978-142446391-6, DOI: 10.1109/ISIE.2010.5636559.

Transformerless Photovoltaic Systems Using Neutral Point Clamped Multilevel Inverters

K. C. Oliveira*, M. C. Cavalcanti*, J. L. Afonso**, A. M. Farias*, F. A. S. Neves*
*Department of Electrical Engineering
Federal University of Pernambuco - Recife, PE - Brazil
kleber.oliveira@ufpe.br, marcelo.cavalcanti@ufpe.br, alexandre.farias@rocketmail.com, fneves@ufpe.br
**Department of Industrial Electronics
University of Minho - Guimaraes, Portugal
jla@dei.uminho.pt

Abstract—**In some photovoltaic applications it is possible to remove the transformer of the system in order to reduce losses, cost and size. In transformerless systems the photovoltaic module parasitic capacitance can introduce leakage currents in which the amplitude depends on the converter topology, on the pulse-width-modulation and on the resonant circuit composed by the system components. In this paper a modulation technique for three-phase neutral point clamped multilevel inverters is proposed to eliminate the leakage current in photovoltaic systems without requiring any modification on the multilevel inverter. The neutral point clamped inverter is studied for systems with function of active filter using the p-q theory. The proposed system presents control of the maximum power point and compensation of current harmonics and reactive power.**

I. INTRODUCTION

Most of the topologies for photovoltaic (PV) systems have a transformer that adjust the dc voltage input for the inverter and isolates the PV panels from the grid [1][2]. The transformer can be used in line or high frequency, but the line frequency transformer has large size and weight. The high frequency transformer is used in PV systems with some stages, decreasing the efficiency and making the system more complex [3]-[5]. The main disadvantage of the topologies without transformer is the connection of the PV array to the grid without galvanic isolation, that rises the leakage current through the parasitic capacitance of the PV array. Due to this capacitance and depending on the inverter topology and the switching strategy, fluctuations of the potential between the PV array and ground can appear. These fluctuations inject a capacitive leakage current and this current can cause grid current distortion, losses in the s ystem and safety problems [5]. In standard topologies, high currents appear because of the conventional pulse-width-modulation (PWM) and three-phase inverters are not suitable for transformerless PV applications.

Some works show alternatives of PWM to reduce the common-mode voltage (CMV) [6]-[8] for electrical machines and it is not necessary to keep the CMV constant. The reduction in the CMV presented in [7] eliminates a vector that would be applied in the switching period. In [8], the vectors that are applied in a switching period are chosen in such a way to keep the CMV constat in this interval. The same result is obtained in [6], where the proposed PWM, called 1DM, generates a voltage reference applying the nearest vectors to make the calculation of the switching times.

In PV systems where series PV arrays are connected to a conventional two-level inverter, the occurrence of partial shades and the mismatching of the arrays leads to a reduction of the generated power [9][10]. To overcome these problems, the connection of the arrays can be made using a multilevel converter [11]-[13]. The multilevel converter maximizes the power obtained from the arrays, reduces the device voltage stress and generates a lower output voltage harmonic distortion [11]. Studying the three basic topologies of the multilevel inverters (neutral point clamped (NPC), cascaded and flying capacitor), the NPC topology was chosen mainly due to its characteristics of easing control, specially when compared to the flying capacitor topology that has a difficult voltage control of the clamping capacitors. In this paper, a modulation technique for three-phase NPC multilevel inverters is proposed to eliminate the leakage current in transformerless photovoltaic systems without requiring any modification on the multilevel inverter and any additional hardware.

On the other hand, it was proposed in 1983 a new theory for the control of active filters in three-phase power systems called p-q theory [14][15]. The theory was initially developed for three-phase three-wire systems, with a brief mention to systems with neutral wire. Later, the theory was extended to three-phase four-wire systems [16][17]. Since the p-q theory is based on the time domain, it is valid both for steady-state and transient operation, as well as for generic voltage and current waveforms, allowing the control of the active filters in real-time. In this paper a transformerless photovoltaic topology using neutral point clamped inverters is studied for systems with function of active filter using the p-q theory.

II. PHOTOVOLTAIC SYSTEM CONTROL

The PV system control uses the p-q theory. This theory makes the transformation of the stationary reference in *abc* coordinates for the reference in α-β-0 coordinates.

A. p-q Theory

The transformations applied to the line voltages and load currents are given by:

978-1-4244-6392-3/10/$26.00 ©2010 IEEE

$$\begin{bmatrix} v_\alpha \\ v_\beta \\ v_0 \end{bmatrix} = \sqrt{\frac{2}{3}} \cdot \begin{bmatrix} 1 & -\frac{1}{2} & -\frac{1}{2} \\ 0 & \frac{\sqrt{3}}{2} & -\frac{\sqrt{3}}{2} \\ \frac{1}{\sqrt{2}} & \frac{1}{\sqrt{2}} & \frac{1}{\sqrt{2}} \end{bmatrix} \cdot \begin{bmatrix} v_a \\ v_b \\ v_c \end{bmatrix} \tag{1}$$

$$\begin{bmatrix} i_\alpha \\ i_\beta \\ i_0 \end{bmatrix} = \sqrt{\frac{2}{3}} \cdot \begin{bmatrix} 1 & -\frac{1}{2} & -\frac{1}{2} \\ 0 & \frac{\sqrt{3}}{2} & -\frac{\sqrt{3}}{2} \\ \frac{1}{\sqrt{2}} & \frac{1}{\sqrt{2}} & \frac{1}{\sqrt{2}} \end{bmatrix} \cdot \begin{bmatrix} i_a \\ i_b \\ i_c \end{bmatrix} \tag{2}$$

These transformations have the advantage of allowing to separate the zero sequence components (v_0 and i_0) present in the voltages and currents. With the voltages and currents determined in α-β-0 coordinates, the real power (p), the imaginary power (q) and zero sequence power (p_0) can be calculated using the p-q theory:

$$\begin{bmatrix} p \\ q \\ p_0 \end{bmatrix} = \begin{bmatrix} v_\alpha & v_\beta & 0 \\ -v_\beta & v_\alpha & 0 \\ 0 & 0 & v_0 \end{bmatrix} \cdot \begin{bmatrix} i_\alpha \\ i_\beta \\ i_0 \end{bmatrix} \tag{3}$$

where:

$$\begin{aligned} p &= v_\alpha \cdot i_\alpha + v_\beta \cdot i_\beta && (4) \\ q &= -v_\beta \cdot i_\alpha + v_\alpha \cdot i_\beta && (5) \\ p_0 &= v_0 \cdot i_0 && (6) \end{aligned}$$

It is possible to separate the power components in average and alternating values [18]:

- $\bar{p}$ - Average value of the real power.
- $\tilde{p}$ - Alternating value of the real power.
- $\bar{q}$ - Average value of the imaginary power.
- $\tilde{q}$ - Alternating value of the imaginary power.
- $\bar{p_0}$ - Average value of the zero sequence power.
- $\tilde{p_0}$ - Alternating value of the zero sequence power.

The three-phase instantaneous power (p_3) corresponds to the sum of the instantaneous real power and the zero sequence power, being given by

$$\begin{aligned} p_3 &= v_\alpha \cdot i_\alpha + v_\beta \cdot i_\beta + v_0 \cdot i_0 && (7) \\ &= p + p_0 && (8) \end{aligned}$$

The zero sequence power only exist if the system presents zero sequence voltage and current. Therefore, if voltage or current does not have zero sequence component, p_3 is numerically equal to p.

The instantaneous imaginary power can be understood as a power that flows among the three phases of the electrical system and does not produce work.

The power q differs of the conventional three-phase reactive power, since all harmonics of voltage and current are also considered. It can be verified that p and q do not depend of the zero sequence voltage and current. Therefore they can be written as:

$$\begin{bmatrix} p \\ q \end{bmatrix} = \begin{bmatrix} v_\alpha & v_\beta \\ -v_\beta & v_\alpha \end{bmatrix} \cdot \begin{bmatrix} i_\alpha \\ i_\beta \end{bmatrix} \tag{9}$$

B. Control of the dc Link Voltage

The dc link control has to keep the capacitors voltages in adequate levels, allowing the inverter to work correctly. In addition to the components of instantaneous power defined by p-q theory, there is also a component, p_{reg}, which is used to adjust the voltage of dc bus capacitors. In the NPC inverter, the dc link has two capacitors and the superior capacitor is charged in the positive semi-cycle of the grid voltage, when it can absorb energy from the supply. The inferior capacitor is charged in the negative semi-cycle of the grid voltage. Therefore two regulation powers p_{reg} are defined: one to charge the superior capacitor in the positive semi-cycle of the grid voltage and the other to charge the inferior capacitor in the negative semi-cycle of the grid voltage. The regulation power (p_{reg}) can be obtained using a proportional controller K_p:

$$\begin{aligned} p_{reg_1} &= K_p \cdot (v_{ref} - V_{dc_1}) && (10) \\ p_{reg_2} &= K_p \cdot (v_{ref} - V_{dc_2}) && (11) \end{aligned}$$

where:

- K_p - proportional gain;
- v_{ref} - reference voltage;
- V_{dc_1} - upper capacitor measured voltage;
- V_{dc_2} - lower capacitor measured voltage.

The total regulation power p_{reg} is:

$$p_{reg} = p_{reg_1} + p_{reg_2} \tag{12}$$

where p_{reg_1} only exist in the positive semi-cycle and p_{reg_2} in the negative semi-cycle of the grid voltage. Therefore when one exists, the other is null. p_{reg} is included with negative signal in the value of real power to be compensated (p_x):

$$\begin{aligned} p_x &= \tilde{p} - \bar{p_0} - p_{reg} && (13) \\ q_x &= q && (14) \end{aligned}$$

C. Currents Control

The undesired power components p_x and q_x are used to calculate the compensation currents in α-β-0 coordinates by expression:

$$\begin{bmatrix} i^*_{c\alpha} \\ i^*_{c\beta} \end{bmatrix} = \frac{1}{v_\alpha^2 + v_\beta^2} \cdot \begin{bmatrix} v_\alpha & -v_\beta \\ v_\beta & v_\alpha \end{bmatrix} \cdot \begin{bmatrix} p_x \\ q_x \end{bmatrix} \tag{15}$$

$$i^*_{c0} = i_0 = \frac{1}{\sqrt{3}} \cdot (i_a + i_b + i_c) \tag{16}$$

Equation (15) is valid when there is not sequence zero power, allowing to select the compensation value (p_0, $\overline{p}_0$ and $\widetilde{p}_0$ or even a parcel of these powers). The block diagram of the control system is presented in Fig. 1.

III. NEUTRAL POINT CLAMPED INVERTER

In order to validate the control system for the NPC topology, the single-phase NPC leg connected to the grid is tested as an inverter. In fact, the three-phase NPC topology can be obtained using three independent single-phase inverters, like the one shown in Fig. 2, connected through the common neutral.

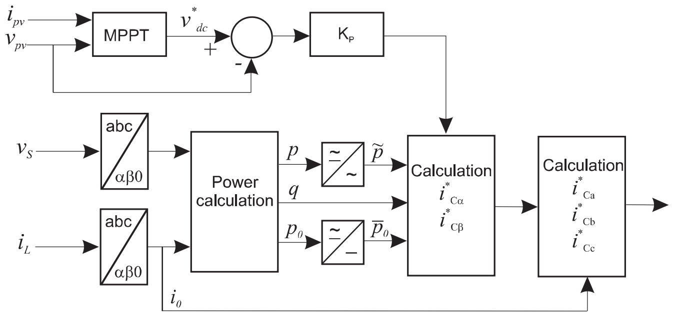

Fig. 1. Block diagram of the control system.

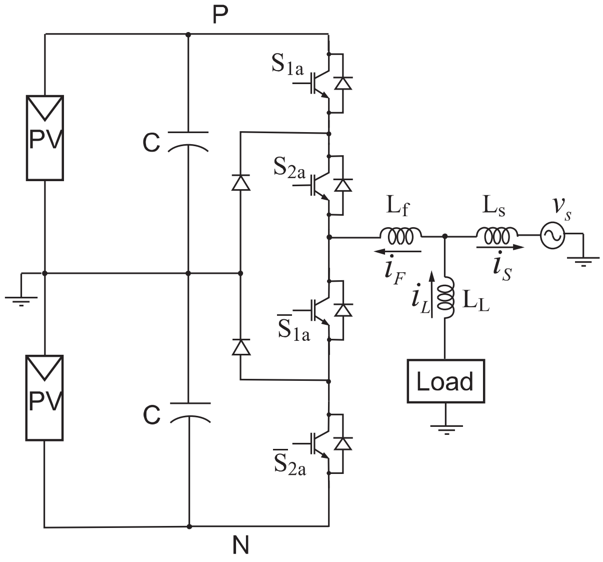

Fig. 2. Single-phase NPC inverter.

A. Single-phase Inverter

The p-q theory was defined exclusively for three-phase systems, but it is possible to consider the single-phase system as part of a balanced three-phase system. In [19], it was shown that using a computational algorithm, the values of the other two phases can be estimated. The method consists of creating two virtual currents (i_b and i_c) and voltages (v_b and v_c) displaced of 120° and 240°, respectively, with the same amplitude of the measured current and voltage, having a virtual three-phase system. The calculations for the virtual three-phase system are the same of a real three-phase system, but only one of the three compensation currents (i^*_{ca}) is used as reference for the control of the active filter. Therefore, the virtual three-phase system is effective in a single-phase system.

The proposed control system with function of active filter using the p-q theory discussed in section II is applied to the single-phase NPC leg connected to the grid. The single-phase control is a adaptation of the three-phase control. The simulation conditions for the single-phase NPC topology are: switching period $T_s = 100\mu s$, source frequency $f = 50Hz$, filter inductance $L_F = 2.35mH$, source voltage $V_S = 115V(rms)$ and dc link capacitance $C = 2.35mF$. Two load conditions were tested in simulation: a load composed of one resistance (25 Ω) and two inductances (50 mH each) with all elements in parallel and a load composed of a rectifier. The simulation results of the load (i_L) and filter (measured - i_F and reference - i^*_{Ca}) currents for the two conditions are presented in Fig. 3. Figure 3(a) shows the results for the linear load in such a way that the control only needs to compensate the power factor making the supply current in phase with the supply voltage. In Figure 3(b), the control is used to compensate harmonics.

In order to verify the simulation results, an experimental setup has been done, which is made up of a single-phase NPC leg connected to the grid, tested as an inverter. The experimental results are presented in Fig. 4. In the first experiment, it is used a linear load in such a way that the control only needs to compensate the power factor making the supply current in phase with the supply voltage (Fig. 4(a)). The second experiment uses the rectifier load and it is necessary to compensate current harmonics (Fig. 4(b)).

In the simulation and experimental results the neutral point balancing issue was considered using the subsection IIb. The dc link voltages were controlled in 200 V for each capacitor, having a total reference of 400 V.

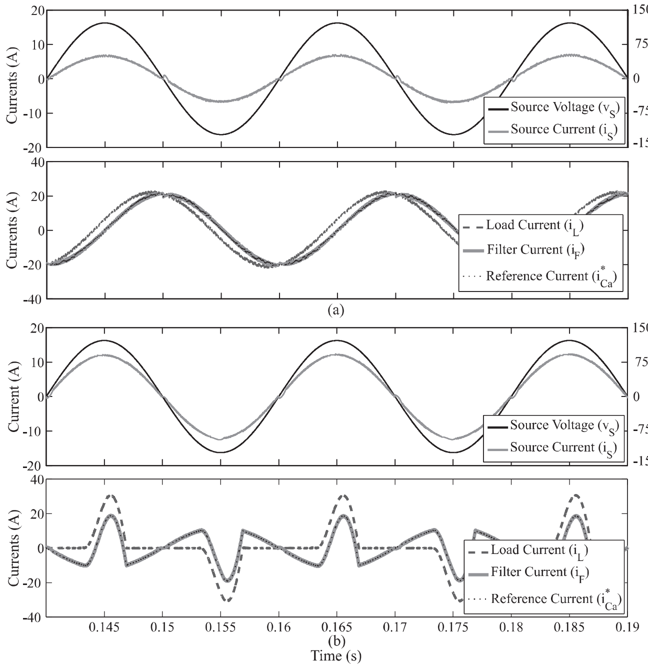

Fig. 3. Simulation results: (a) linear load and (b) non-linear load.

B. Three-phase Inverter

The simulation conditions for the three-phase NPC topology (Fig. 5) are the same of the single-phase NPC inverter. Two load conditions were tested in simulation: a load composed of one resistance (25 Ω) and two inductances (50 mH each) with all elements in parallel for each phase and a load composed of a three-phase rectifier. The simulation results of the load (i_L)

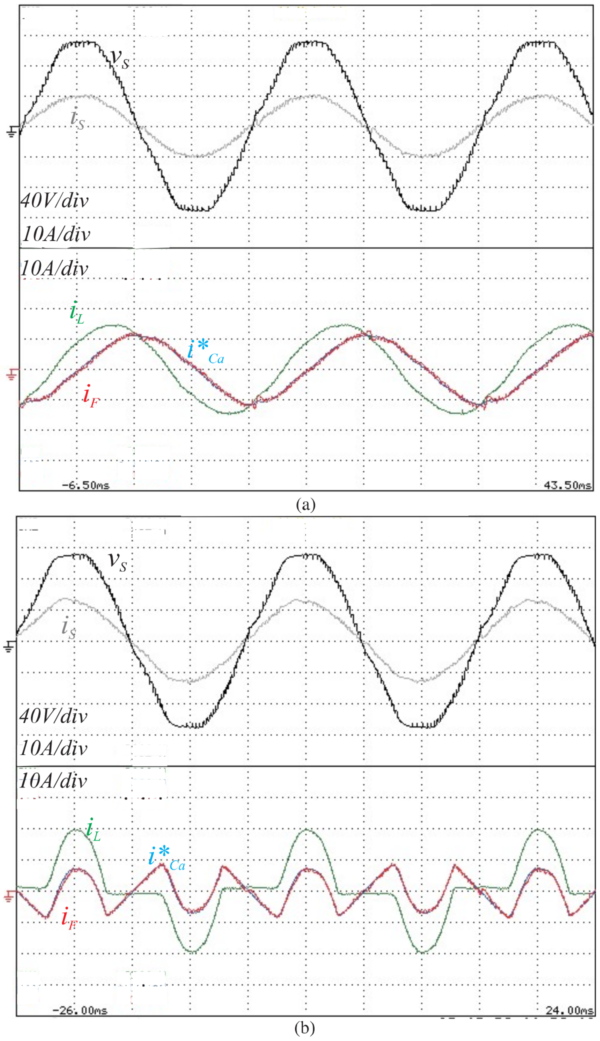

(a)

(b)

Fig. 4. Experimental results: (a) linear load and (b) non-linear load.

and filter (measured - i_F and reference - i^*_{Ca}) currents for the two conditions are presented in Fig. 6. Figure 6(a) shows the results for the linear load in such a way that the control only needs to compensate the power factor making the supply current in phase with the supply voltage. In Figure 6(b), the control is used to compensate harmonics.

IV. Modulation Techniques to Eliminate Leakage Currents in Three-level Inverters

For the transformerless grid connected PV systems, there is a galvanic connection between the grid and the dc source and thus a leakage current appears due to a resonant circuit that is created if the PV array is grounded [3][4]. This resonant circuit includes the PV array stray capacitance, the filter and grid inductances, the inverter stray capacitances and the inductance between the ground connection of the inverter and the grid. The magnitude of the PV array leakage capacitance depends on weather conditions, changing from nF up to μF [5]. Therefore, leakage current can reach high values becoming an important issue in transformerless PV systems.

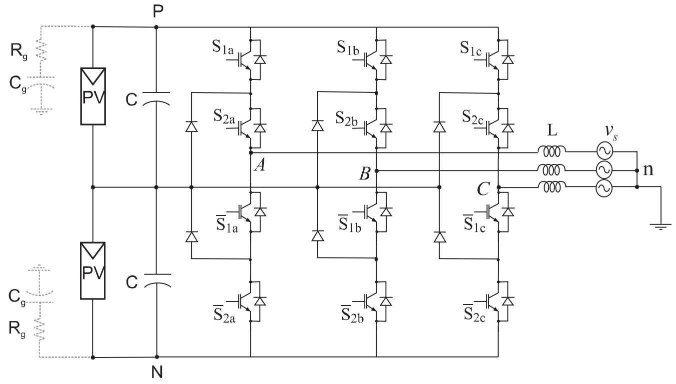

Fig. 5. Three-phase NPC inverter.

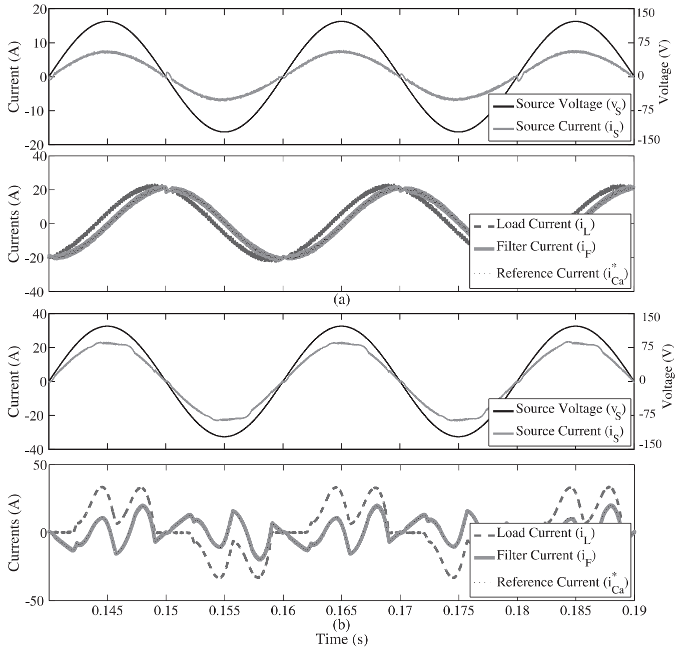

(a)

(b)

Fig. 6. Simulation results to phase a: (a) linear load and (b) non-linear load.

A. Leakage Currents in Three-level Inverters

It is possible to express the leakage voltage (voltage between the positive (P) or negative (N) dc bus and the neutral (n) - V_{Pn} or V_{Nn}) in terms of the inverter output voltages:

$$V_{Nn} = V_{kn} - V_{kN} \tag{17}$$

$$V_{Pn} = V_{kn} - V_{kP} = V_{kn} - (V_{kN} - V_{PN}), \tag{18}$$

where $k = A, B, C$ (Fig. 5).

Under balanced operating conditions, the following condition for the inverter voltages can be written:

$$V_{An} + V_{Bn} + V_{Cn} = 0 \tag{19}$$

Using (17), (18) and (19),

$$V_{Nn} = -\frac{V_{AN}+V_{BN}+V_{CN}}{3} \quad (20)$$

$$V_{Pn} = V_{PN} - \frac{V_{AN}+V_{BN}+V_{CN}}{3} \quad (21)$$

The CMV for the three-phase inverter can be calculated as:

$$V_{CM} = \frac{V_{AN}+V_{BN}+V_{CN}}{3}. \quad (22)$$

The leakage voltage V_{Nn} is the negative of the CMV and the leakage voltage V_{Pn} is $V_{PN} + V_{Nn}$. Therefore the leakage currents can be attenuated by the control of the CMV.

B. Modulation to Eliminate Leakage Currents

The space vector PWM (SVPWM) is generally used to control the three-level inverter output voltages and there are nineteen possible space vectors as shown in Fig. 7: one zero vector (V_0) with three switching possibilities, six long vectors (V_1, V_2, V_3, V_4, V_5 and V_6), six medium vectors (V_7, V_8, V_9, V_{10}, V_{11} and V_{12}) and six small vectors (V_{13}, V_{14}, V_{15}, V_{16}, V_{17} and V_{18}) with two switching possibilities for each one, totalizing twenty-seven possible combinations of voltage. Table I presents the space vectors associated to the possibilities of the inverter switches for the first 150° of the plane α-β and the total CMV for the three-level inverter using (22).

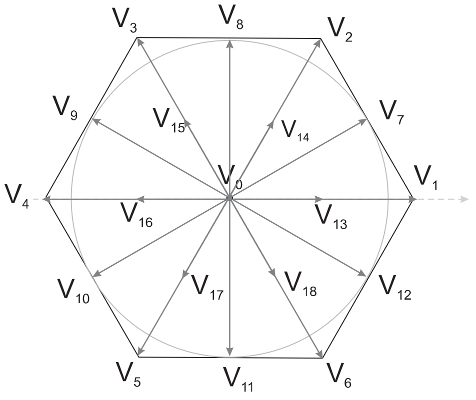

Fig. 7. Space vectors in the output of a three-level inverter.

The proposed technique consists in using only the medium vectors and the zero vector with $V_{CM} = V_{PN}/2$ to compose the reference vector. Therefore, in the region between the vectors V_2 and V_8, the vectors V_7, V_8 and V_0 (with $V_{CM} = V_{PN}/2$) are used. Other option is to use always three medium vectors. Considering the same region, the vectors V_7, V_8 and V_9 could be used in this case. In any option, it can be seen that the CMV always assumes the value $V_{PN}/2$. For the three-level inverters, the proposed PWM can be applied with the maximum amplitude of the phase-to-neutral voltages equal to $V_{PN}/2$, resulting in 86.6% of the voltages that can be obtained with the SVPWM ($V_{PN}/\sqrt{3}$). There are other combinations that guarantee a constant CMV using long and small vectors, but in this case the amplitude of the output voltages will be lower than the amplitude of the voltages using the technique with medium vectors if sinusoidal voltages are desired.

TABLE I

CORRESPONDING SPACE VECTOR FOR THE POSSIBLE COMBINATIONS OF THE INVERTER SWITCHES FOR THE FIRST 150^0.

S_{1a}	S_{2a}	S_{1b}	S_{2b}	S_{1c}	S_{2c}	Vector	V_{CM}
0	0	0	0	0	0	V_0	0
1	1	1	1	1	1	V_0	V_{PN}
0	1	0	1	0	1	V_0	$V_{PN}/2$
1	1	0	0	0	0	V_1	$V_{PN}/3$
1	1	1	1	0	0	V_2	$2V_{PN}/3$
0	0	1	1	0	0	V_3	$V_{PN}/3$
1	1	0	1	0	0	V_7	$V_{PN}/2$
0	1	1	1	0	0	V_8	$V_{PN}/2$
0	0	1	1	0	1	V_9	$V_{PN}/2$
0	1	0	0	0	0	V_{13}	$V_{PN}/6$
1	1	0	1	0	1	V_{13}	$2V_{PN}/3$
0	1	0	1	0	0	V_{14}	$V_{PN}/3$
1	1	1	1	0	1	V_{14}	$5V_{PN}/6$
0	0	0	1	0	0	V_{15}	$V_{PN}/6$
0	1	1	1	0	1	V_{15}	$2V_{PN}/3$

V. COMPARATIVE ANALYSIS

In this section, transformerless PV three-phase inverters (Fig. 5) using different PWM techniques are compared based on the output voltages amplitude, CMV and leakage currents. The simulation parameters are: switching period $T_s = 100\mu s$, source frequency $f = 50Hz$, source inductance $L = 4.5mH$, source voltage $V_S = 110V(rms)$, dc link voltage $V_{PN} = 650V$, modulation index $m = 0.8$, parasitic capacitance $C_g = 470nF$ and ground resistance $R_g = 25\Omega$. Simulation results for the leakage currents are presented in Fig. 8 for different PWM techniques. In this figure, the proposed solution is compared to the solution proposed to solve the problem for electrical machines. For transformerless PV applications, it is necessary to keep the CMV constant to reduce the leakage currents. The results in Fig. 8 show that using the proposed PWM, the three-level inverters present low leakage currents in transformerless PV systems. Figure 9 shows the results for the inverter output voltage and grid (source) current in phase a for 1DM and proposed PWM. It can be seen that the current waveform is not distorted when compared with other PWM techniques.

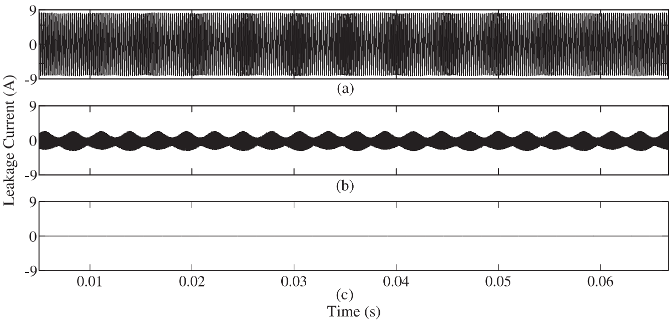

Fig. 8. Simulated leakage current of the three-level PV inverter: (a) SVPWM, (b) 1DM, (c) proposed PWM (medium vectors).

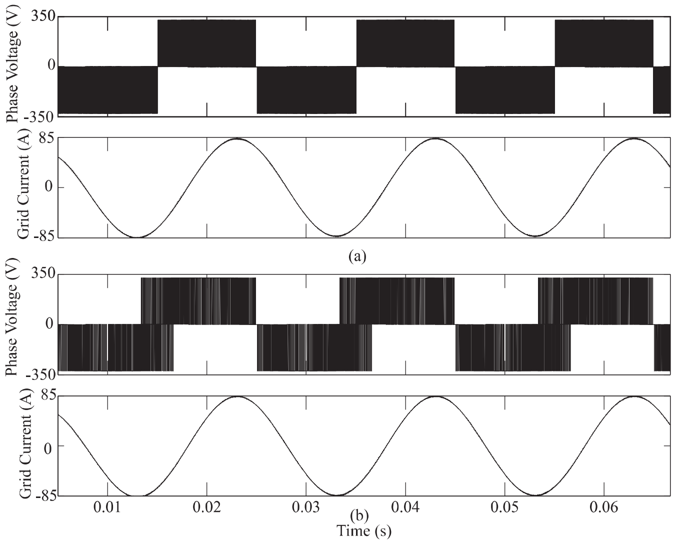

Fig. 9. Output voltage and grid current in phase *a* for (a) 1DM and (b) proposed PWM.

The comparison is shown in Table II. Using SVPWM or 1DM, the PV array terminals are jumping between different levels with the switching frequency resulting in high leakage currents. Considering the leakage current, the three-level inverters are suitable in case of applying the proposed technique. The total harmonic distortion (THD) is defined as:

$$THD = \sqrt{\frac{\sum_{h=2}^{\infty} F_h^2}{F_1^2}} 100\%, \qquad (23)$$

where F_h is the rms value of each frequency component of the inverter output current.

TABLE II
COMPARISON OF TRANSFORMERLESS THREE-PHASE INVERTERS.

PWM	SVPWM	1DM	Proposed
Voltage amplitude	$V_{PN}/\sqrt{3}$	$V_{PN}/\sqrt{3}$	$V_{PN}/2$
CM voltage	variable	variable	constant
Leakage current	high	medium	low
THD Current	1.77	1.66	1.54

VI. CONCLUSION

In this paper, a control system with function of active filter using the p-q theory is discussed. The neutral point clamped inverter is studied for single-phase and three-phase systems, being presented simulation and experimental results. A modulation technique designed for three-phase transformerless photovoltaic systems is proposed. The technique guarantee constant common-mode voltage, improving the behavior of the three-level inverters in terms of leakage currents without additional hardware.

ACKNOWLEDGMENT

The authors would like to thank CNPq, ERASMUS MUNDUS and ISAC for the financial suport.

REFERENCES

[1] F. Blaabjerg, R. Teodorescu, M. Liserre, A.V. Timbus, “Overview of Control and Grid Synchronization for Distributed Power Generation Systems”, *IEEE Transactions on Industrial Electronics*, vol. 53, no. 5, October 2006, pp. 1398-1409.

[2] M. Liserre, A. Pigazo, A. Dell’Aquila, V.M. Moreno, “An Anti-Islanding Method for Single-Phase Inverters Based on a Grid Voltage Sensorless Control”, *IEEE Transactions on Industrial Electronics*, vol. 53, no. 5, October 2006, pp. 1418-1426.

[3] T. Kerekes, R. Teodorescu, M. Liserre, “Common Mode Voltage in case of Transformerless PV Inverters Connected to the Grid”, in *IEEE International Symposium on Industrial Electronics*, June, 2008, pp. 2390 -2395.

[4] E. Gubía, P. Sanchis, A. Ursúa, J. López, L. Marroyo, “Ground currents in single-phase transformerless photovoltaic systems”, *Progress in Photovoltaics: Research and Applications*, vol. 15, no. 7, November 2007, pp. 629-650.

[5] O. Lopez, R. Teodorescu, F. Freijedo, J. Doval-Gandoy, “Eliminating ground current in a transformerless photovoltaic application”, in *Power Engineering Society General Meeting, 2007. IEEE*, June, 2007, pp. 1 - 5.

[6] J. Leon, S. Vazquez, J. Sanchez, R. Portillo, L. Franquelo, J. Carrasco, E. Dominguez, “Conventional Space-Vector Modulation Techniques versus the Single-Phase Modulator for Multilevel Converters”, *IEEE Transactions on Industrial Electronics*, 2010.

[7] A. Virtanen, M. Jussila, H. Tuusa, “Comparison of common-mode voltages in frequency converters with alternative space vector modulation methods”, *IEEE Power Electronics Specialists Conference*, vol. 53, no. 5, june 2008, pp. 2248 -2256.

[8] M. Renge, M. Suryawanshi, ”Three-Dimensional Space Vector Modulation to Reduce Common-Mode Voltage for Multilevel Inverter”, *IEEE Transactions on Industrial Electronics*, 2010.

[9] M. García, J.M. Maruri, L. Marroyo, E. Lorenzo, M. Pérez, “Partial shadowing, MPPT performance and inverter configurations: observations at tracking PV plants”, *Progress in Photovoltaics: Research and Applications*, vol. 16, no. 6, September 2008, pp. 529-536.

[10] P. Sanchis, J. López, A. Ursúa, E. Gubía, L. Marroyo, “On the testing, characterization, and evaluation of PV inverters and dynamic MPPT performance under real varying operating conditions”, *Progress in Photovoltaics: Research and Applications*, vol. 15, no. 6, September 2007, pp. 541-556.

[11] S. Busquets-Monge, J. Rocabert, P. Rodriguez, S. Alepuz, J. Bordonau, “Multilevel Diode-Clamped Converter for Photovoltaic Generators With Independent Voltage Control of Each Solar Array”, *IEEE Transactions on Industrial Electronics*, vol. 55, no. 7, July 2008, pp. 2713-2723.

[12] R. Gonzalez, E. Gubia, J. Lopez, L. Marroyo, “Transformerless Single-Phase Multilevel-Based Photovoltaic Inverter”, *IEEE Transactions on Industrial Electronics*, vol. 55, no. 7, July 2008, pp. 2694-2702.

[13] S. Daher, J. Schmid, F.L.M. Antunes, “Multilevel Inverter Topologies for Stand-Alone PV Systems”, *IEEE Transactions on Industrial Electronics*, vol. 55, no. 7, July 2008, pp. 2703-2712.

[14] H. Akagi, Y. Kanazawa, A. Nabae, “Generalized Theory of the Instantaneous Reactive Power in Three-phase Circuits”, Int. Power Electronics Conf., 1983, pp. 1375-1386.

[15] H. Akagi, Y. Kanazawa, A. Nabae, “Instanataneous Reactive Power Compensator Comprising Switching Devices without Energy Storage Components”, *IEEE Transactions on Industry Applications*, vol. 20, no. 3, May/June 1984, pp. 625 - 630.

[16] E.H. Watanabe, R.M. Stephan, M. Aredes, “New Concepts of Instantaneous Active and Reactive Powers in Electrical Systems with Generic Loads”, *IEEE Transactions on Power Delivery*, vol. 8, no. 2, April 1993, pp. 697-703.

[17] M. Aredes, E.H. Watanabe, “New Control Algorithm for Series and Shunt Three-phase Four-Wire Active Power Filters”, *IEEE Transactions on Power Delivery*, vol. 10, no. 3, July 1995. pp. 1619-1656.

[18] J.L. Afonso, M.J.S. Freitas, J.S. Martins, “p-q Theory Power Components Calculations”, *IEEE International Symposium on Industrial Electronics*, vol. 1, June 2003, pp. 385-390.

[19] J. Liu, J. Yang, Z. Wang, “A new approach for single-phase harmonic current detecting and its application in a hybrid active power filter”, *Proceedings on Industrial Electronics Society Conference*, vol.2, July 1999, pp. 849-854.